

# Cationic Ring-Opening Polymerization of 2-Propyl-2-oxazolines: Understanding Structural Effects on Polymerization Behavior Based on Molecular Modeling

Hannelore Goossens,<sup>†</sup> Saron Catak,<sup>†</sup> Mathias Glassner,<sup>‡</sup> Victor R. de la Rosa,<sup>‡</sup> Bryn D. Monnery,<sup>‡</sup> Frank De Proft,<sup>§</sup> Veronique Van Speybroeck,<sup>\*,†</sup> and Richard Hoogenboom<sup>\*,‡</sup>

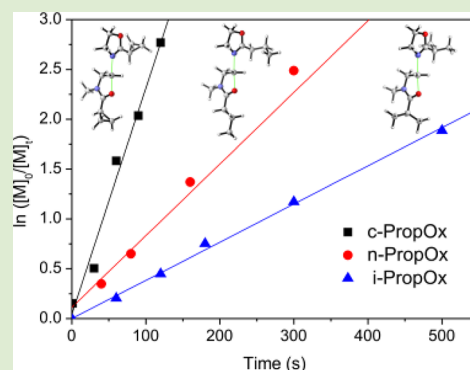
<sup>†</sup>Center for Molecular Modeling, Ghent University, Technologiepark 903, 9052 Zwijnaarde, Belgium

<sup>‡</sup>Supramolecular Chemistry Group, Department of Organic Chemistry, Ghent University, Krijgslaan 281-S4, 9000 Ghent, Belgium

<sup>§</sup>Eenheid Algemene Chemie, Vrije Universiteit Brussel, Pleinlaan 2, 1050 Brussels, Belgium

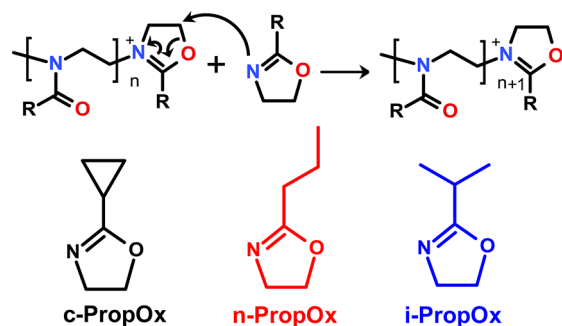
## Supporting Information

**ABSTRACT:** The surprising difference in the cationic ring-opening polymerization rate of 2-cyclopropyl-2-oxazoline versus 2-*n*-propyl-2-oxazoline and 2-isopropyl-2-oxazoline was investigated both experimentally and theoretically. The polymerization kinetics of all three oxazolines were experimentally measured in acetonitrile at 140 °C, and the polymerization rate constant ( $k_p$ ) was found to decrease in the order *c*-PropOx > *n*-PropOx > *i*-PropOx. Theoretical free energy calculations confirmed the trend for  $k_p$ , and a set of DFT-based reactivity descriptors, electrostatics, and frontier molecular orbitals were studied to detect the factors controlling this peculiar behavior. Our results show that the observed reactivity is dictated by electrostatic effects. More in particular, the charge on the nitrogen atom of the monomer, used to measure its nucleophilicity, was the most negative for *c*-PropOx. Furthermore, the electrophilicity of the cations does not change substantially, and thus, the nucleophilicity of the monomers is the driving factor for  $k_p$ .



Poly(2-oxazoline)s are synthetic polyamides that are regaining interest in the past decade because of their synthetic versatility in combination with an excellent biocompatibility.<sup>1</sup> The synthetic versatility results from their preparation via living cationic ring-opening polymerization (CROP), providing direct access to well-defined (co)-polymers.<sup>2</sup> In addition, a wide range of monomers can be prepared and utilized in CROP to tune the polymer properties.<sup>3</sup> Poly(2-propyl-2-oxazoline) (poly(PropOx)) (co)-polymers are of special interest due to their thermoresponsive phase transitions, i.e., lower critical solution temperature behavior, in aqueous solution.<sup>4</sup> We recently introduced poly(2-cyclopropyl-2-oxazoline) (poly(*c*-PropOx)) as an alternative for poly(2-isopropyl-2-oxazoline) (poly(*i*-PropOx)) and poly(2-*n*-propyl-2-oxazoline) (poly(*n*-PropOx)) (see Scheme 1 for monomer structures). It was demonstrated that poly(*c*-PropOx) has a higher glass transition temperature than poly(*n*-PropOx). Moreover, it is amorphous, preventing the irreversible crystallization upon thermal annealing as found for poly(*i*-PropOx).<sup>5</sup> This study surprisingly revealed that the CROP of *c*-PropOx was twice as fast as that of *n*-PropOx. Furthermore, Kataoka reported that *n*-PropOx is incorporated faster than *i*-PropOx during statistical copolymerizations,<sup>4b</sup> although a direct comparison of homopolymerization rates has not been reported. Hence, it might be speculated that the reactivity for

**Scheme 1. Overview of the Propagation Step of the Cationic Ring-Opening Polymerization of 2-Oxazolines (Top) and Structures of the Three Investigated 2-Propyl-2-oxazoline Monomers (Bottom)**



the CROP of PropOx decreases in the order *c*-PropOx > *n*-PropOx > *i*-PropOx.

Herein we have performed an experimental and computational study to gain insight into the effect of the side chain structure of PropOx on the reactivity for CROP. In general, the

Received: June 7, 2013

Accepted: July 10, 2013

Published: July 16, 2013

propagation step of the CROP of 2-oxazolines occurs by nucleophilic attack of the free electron pair of the endocyclic nitrogen atom on the C5 position of the oxazolinium ring at the end of the living chain (Scheme 1). It can be anticipated that both the nucleophilicity of the monomer and the electrophilicity of the oxazolinium species are important parameters for the speed of the CROP. However, they are influenced by the electronic properties of the side chain substituent in an opposite manner: a more electron-donating side chain will enhance the nucleophilicity of the monomer while stabilizing the oxazolinium cation, making it less electrophilic, and vice versa for a less electron-donating side chain. Most literature data for CROP of 2-oxazolines suggest that decreasing the reactivity of the cationic living chain ends by enhancing the electron-donating capabilities of the side chain is predominant and leads to a slower polymerization: the polymerization rate constant ( $k_p$ ) for aliphatically substituted monomers decreases in the order 2-methyl-2-oxazoline > 2-ethyl-2-oxazoline > *i*-PropOx,<sup>4b,6</sup> while the  $k_p$  for aromatically substituted monomers decreases in the order 2-(4-nitrophenyl)-2-oxazoline > 2-phenyl-2-oxazoline > 2-(4-methoxy-phenyl)-2-oxazoline.<sup>7</sup> However, opposing results have also been reported, i.e., the very slow polymerization of 2-fluoroalkyl-2-oxazolines<sup>8</sup> and the very fast polymerization of 2-(2,6-difluorophenyl)-2-oxazoline,<sup>9</sup> which was ascribed to loss of conjugation. On the other hand, a number of well-known “traditional” solution acidity and basicity sequences are inverted in the gas phase, giving the impression that alkyl groups act as electron-withdrawing species.<sup>10</sup> It is clear that a thorough theoretical investigation is needed to get a better insight into the effects of the monomer structure on the  $k_p$  for CROP. In this letter, we focus on *c*-PropOx, *n*-PropOx, and *i*-PropOx.

To facilitate a direct comparison, the polymerization kinetics of all three PropOx monomers were investigated under the same, previously optimized, conditions, namely, in acetonitrile with 4 M monomer concentration and methyl tosylate as initiator (monomer to initiator ratio of 50) at 140 °C under microwave irradiation, which does not influence  $k_p$  compared to thermal heating.<sup>6</sup> The first-order kinetic plot revealed a linear increase of  $\ln([M]_0/[M]_t)$  with time for all three monomers demonstrating that no termination occurred. Furthermore, the number average molecular weight ( $M_n$ ) increased linearly with conversion, while the dispersity ( $\mathcal{D}$ ) remained below 1.20 (see Figure S1 of the Supporting Information). As such, it can be concluded that all three polymerizations proceeded in a living manner.

The first-order kinetic plot (Figure 1) clearly reveals that the polymerization rate strongly changes upon variation of the propyl substituent of the monomer: the polymerization rate decreases in the order *c*-PropOx > *n*-PropOx > *i*-PropOx as was anticipated from the literature data. The  $k_p$  values were calculated from the slope of the first-order kinetic plots (Table 1), revealing that the  $k_p$  of *c*-PropOx is 2–3 times higher than the  $k_p$  of *n*-PropOx and 6 times higher than the  $k_p$  of *i*-PropOx, whereby it should be noted that the  $k_p$  of *c*-PropOx was found to be only reproducible for freshly prepared batches of monomer indicating a not yet understood minor degradation pathway interfering with the polymerization. Furthermore, it was observed that demixing occurs during cooling of the *c*-PropOx polymerization mixture, but polymerization in a pressure reaction tube confirmed homogeneous polymerization at 140 °C (see Figure S2, Supporting Information). Even though the lower reactivity of *i*-PropOx compared to *n*-PropOx

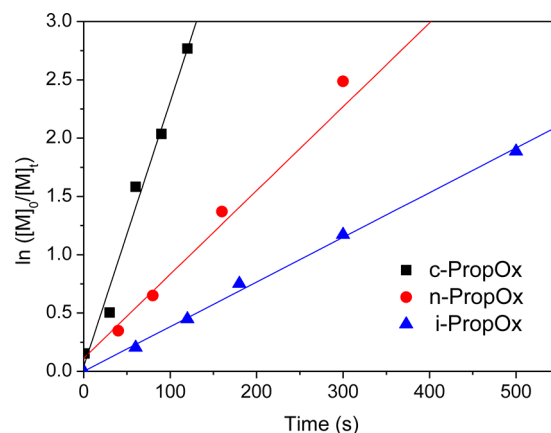


**Figure 1.** First-order kinetic plot for the cationic ring-opening polymerization of *c*-PropOx, *n*-PropOx, and *i*-PropOx. Polymerizations performed at 140 °C in acetonitrile with 4 M monomer (M) concentration, methyl tosylate (I) as initiator, and a  $[M]:[I]$  ratio of 50. *c*-PropOx data from ref 5.

**Table 1.** Experimental and Calculated Polymerization Rate Constants  $k_p$  ( $L \times mol^{-1} \times s^{-1}$ ) and Calculated Free Energies of Activation  $\Delta G^\ddagger$  and Free Reaction Energies  $\Delta G_{rxn}$  (kJ/mol) for the CROP of the Different PropOx Monomers<sup>a,b</sup>

	<i>c</i> -PropOx	<i>n</i> -PropOx	<i>i</i> -PropOx
experimental $k_p$	$0.27 \pm 0.01$	$0.093 \pm 0.002$	$0.048 \pm 0.007$
calculated $k_p$	0.252	0.046	0.003
$\Delta G^\ddagger$	95.4	101.3	110.4
$\Delta G_{rxn}$	-46.0	-34.6	-31.2

<sup>a</sup>Energies were calculated with respect to separate reactants, and BSSE corrections were taken into account. <sup>b</sup>Free energies in kJ/mol at 140 °C and 1 atm.

might be intuitively ascribed to better stabilization of the oxazolinium propagating species by the presence of the isopropyl substituent, the effect of the cyclopropyl substituent cannot be directly rationalized.

To better understand the difference in reactivity for the CROP of *c*-PropOx, *n*-PropOx, and *i*-PropOx, the first propagation step of the CROP of the three species under study, i.e., addition of a 2-oxazoline unit onto a methylated oxazolinium species (see Scheme S1 of the Supporting Information), was investigated by means of DFT calculations.

Preliminary calculations were done with the B3LYP/6-31+G(d,p) level of theory,<sup>11</sup> and energies were refined with several functionals with a 6-31+G(d,p) basis set. The M06-2X functional<sup>12</sup> was found to result in  $k_p$  values in good agreement with the experiments (see Figure S3 of the Supporting Information) and was therefore used for further optimizations. A thorough conformational analysis was performed on all reactants, transition states, and products to identify the most plausible conformers. The stationary points were characterized as minima (ground states) or first-order saddle points (transition states) by normal modes analysis. IRC (intrinsic reaction coordinate) calculations<sup>13</sup> followed by full geometry optimizations were used to verify the corresponding reactant and product complexes. Free energies of activation and corresponding  $k_p$  values were calculated from separate reactants, and BSSE (basis set superposition error) corrections<sup>14</sup> were taken into account. All calculations were carried

out with the Gaussian09 program package<sup>15</sup> at 1 atm and 25 °C, and the results at 140 °C were obtained by using proper thermodynamic corrections.

Transition state geometries for the first propagation step of the CROP of the three species under study are shown in Figure 2. Free energy profiles are shown in Figure S4 of the

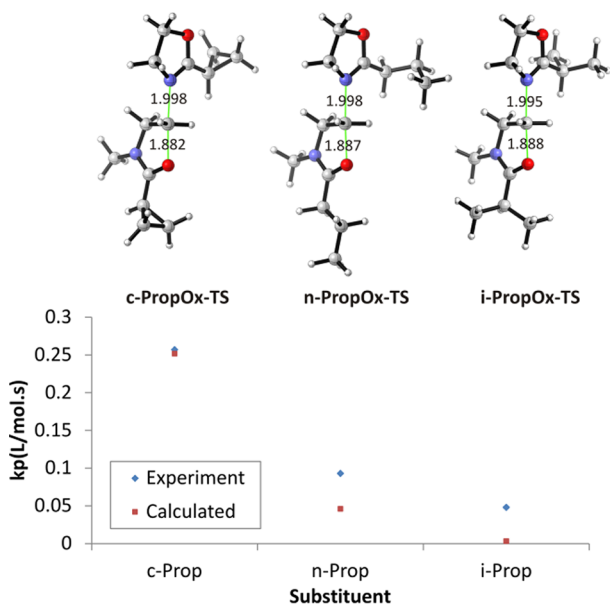


**Figure 2.** Comparison of experimental and calculated (M06-2X/6-31++G(d,p)) rate constants for the first propagation step of the CROP of *c*-PropOx, *n*-PropOx, and *i*-PropOx (Scheme 1 with  $n = 0$ ). Transition state (TS) geometries are shown. The counterion has been omitted in the calculations. Some critical distances are given in Å.

Supporting Information. The experimental trends for the reactivity of the CROP (*c*-PropOx > *n*-PropOx > *i*-PropOx) are nicely reproduced (Table 1). The earliest transition state is found for *c*-PropOx, corresponding to the lowest free energy of activation (95.4 kJ/mol), and the latest transition state is found for *i*-PropOx, corresponding to the highest free energy of activation (110.4 kJ/mol). Furthermore, the lowest reaction energies and hence most stable products (from the first propagation step) are found for *c*-PropOx and vice versa for *i*-PropOx. Moreover, the experimental and calculated  $k_p$  values correspond well (Table 1 and Figure 2). The larger difference between the calculated and the experimental  $k_p$  values for *i*-PropOx (1 order of magnitude) is most probably caused by the computational margin of error (~5 kJ/mol). The effect of the different propyl substituents on the electronic structure of the oxazoline monomer and the oxazolinium cation will be investigated in more detail by analysis of reactivity descriptors, electrostatics, and frontier molecular orbitals.

DFT-based reactivity descriptors are defined as derivatives of the electronic energy  $E[N, \nu(\mathbf{r})]$  with  $N$  being the total number of electrons and  $\nu(\mathbf{r})$  the external potential.<sup>16</sup> The global hardness  $\eta$  can be computed from the vertical ionization potential (IP) and the electron affinity (EA)

$$\eta = \frac{\text{IP} - \text{EA}}{2}$$

The global hardness  $\eta$  of the oxazoline monomers and the oxazolinium cations under study is given in Table 2. All species under study can be considered as intermediate-hard molecules,

**Table 2.** Global Hardness (eV) of the Oxazoline Monomers and the Oxazolinium Cations under Study (M06-2X/6-31++G(d,p))

	monomer	cation
<i>c</i> -PropOx	4.95	5.54
<i>n</i> -PropOx	5.11	5.71
<i>i</i> -PropOx	5.08	5.72

since  $\eta$  values vary from 4.95 to 5.72 eV. Monomers and cations of *c*-PropOx are the softest and therefore most reactive species, according to the principle of maximum hardness.<sup>17</sup>  $\eta$  values for *n*-PropOx and *i*-PropOx are very similar. Since electron-transfer effects favor soft–soft interactions and electrostatic effects favor hard–hard interactions,<sup>18</sup> it can be anticipated that the CROP of *c*-PropOx, *n*-PropOx, and *i*-PropOx is mainly driven by electrostatics. Furthermore, the polymerization occurs due to the nucleophilic attack of a nitrogen atom, which can be considered as a hard atom.

However, local Fukui functions  $f(\mathbf{r})$ ,<sup>19</sup> which can be used to describe orbital-controlled reactions, were calculated too to get a complete picture of the problem at hand. The results are shown in Figure S5 of the Supporting Information. No clear differences are noticed here, and this clearly indicates that the reactions are not driven by frontier orbitals.

Population analysis can be used to gain insight into the electrostatic structure of molecular systems by calculating the net atomic charges using a population scheme. Hirshfeld-I (Iterative Hirshfeld)<sup>20</sup> charges have been shown to be robust toward the basis set and conformational changes and reproduce the ESP (electrostatic potential) around the molecule. The charges of the nitrogen atoms of the monomers and the attacked carbon atoms of the cations are shown in Table 3. The

**Table 3.** Hirshfeld-I Charges (M06-2X/6-31++G(d,p)) of the Oxazoline Monomers and the Oxazolinium Cations under Study

	<i>c</i> -PropOx	<i>n</i> -PropOx	<i>i</i> -PropOx
N monomer	−0.576	−0.555	−0.545
C cation	0.016	0.014	0.011

differences among the three species under study are very small (max. 0.031). The lowest (most negative) charge on the nitrogen atom is found for the *c*-PropOx monomer, and the highest (least negative) charge is found for the *i*-PropOx monomer. This indeed points toward a larger nucleophilicity of the *c*-PropOx monomer and is in line with the fastest polymerization of *c*-PropOx and the slowest polymerization of *i*-PropOx. The differences in attacked carbon atom charges of the cations are negligible, but the small variations are in line with the experimental order of reactivity. Hence, the experimental trend for the reactivity of the CROP of *c*-PropOx, *n*-PropOx, and *i*-PropOx is most probably governed by the charge of the nitrogen atom on the monomers and therefore by the nucleophilicity of the monomers. Calculation of the electrophilicities (see page S4 of the Supporting Information for the definition) of the cations further confirms that they have little influence on the differences in reactivity of the CROP. The electrophilicities of the three cations under study were found to be very similar: 7.18, 7.33, and 7.28 eV for the *c*-PropOx, *n*-PropOx, and *i*-PropOx cations, respectively.



In conclusion, the unexpected difference in the reactivity for the CROP of PropOx has been experimentally determined to be *c*-PropOx > *n*-PropOx > *i*-PropOx. Theoretical calculations reproduced this trend, predicting a higher polymerization rate for *c*-PropOx. A detailed study using various molecular descriptors revealed that the reactivity is mainly controlled by the electrostatics and more in particular by the higher negative charge of the nitrogen atom on the *c*-PropOx monomer, thus pointing toward a higher nucleophilicity of the latter. Further studies will be done to generalize the obtained conclusions.

## ■ ASSOCIATED CONTENT

### ■ Supporting Information

$M_n$  and PDI versus conversion plots, pictures of the *c*-PropOx polymerization mixtures, Cartesian coordinates, energies, and imaginary and low frequencies of the optimized geometries (M06-2X/6-31++G(d,p)) of transition states. This material is available free of charge via the Internet at <http://pubs.acs.org>.

## ■ AUTHOR INFORMATION

### Corresponding Author

\*E-mail: [veronique.vanspeybroeck@ugent.be](mailto:veronique.vanspeybroeck@ugent.be); [richard.hoogenboom@ugent.be](mailto:richard.hoogenboom@ugent.be).

### Notes

The authors declare no competing financial interest.

## ■ ACKNOWLEDGMENTS

The authors are grateful to the Belgium Federal Government for funding via the Interuniversity Attraction Poles scheme 7/05 as well as Ghent University for funding via the Concerted Research Actions scheme and the Research Foundation-Flanders (FWO-Vlaanderen). The computational resources used in this work were provided by Stevin Supercomputer Infrastructure Ghent University (Belgium), the Hercules Foundation, and the Flemish Government – department EWI.

## ■ REFERENCES

- (1) (a) Adams, N.; Schubert, U. S. *Adv. Drug Delivery Rev.* **2007**, *59*, 1504–1520. (b) Schlaad, H.; Diehl, C.; Gress, A.; Meyer, M.; Demirel, A. L.; Nur, Y.; Bertin, A. *Macromol. Rapid Commun.* **2010**, *31*, 511–525. (c) Hoogenboom, R. *Angew. Chem., Int. Ed.* **2009**, *48*, 7978–7994. (d) Luxenhofer, R.; Han, Y.; Schulz, A.; Tong, J.; He, Z.; Kabanov, A. V.; Jordan, R. *Macromol. Rapid Commun.* **2012**, *33*, 1613–1631.
- (2) (a) Kobayashi, S. *Prog. Polym. Sci.* **1990**, *15*, 751–823. (b) Aoi, K.; Okada, M. *Prog. Polym. Sci.* **1996**, *21*, 151–208. (c) Hoogenboom, R. *Macromol. Chem. Phys.* **2007**, *208*, 18–25. (d) Makino, A.; Kobayashi, S. *J. Polym. Sci., Part A: Polym. Chem.* **2010**, *48*, 1251–1270.
- (3) (a) Levy, A.; Litt, M. *J. Polym. Sci., Part B* **1967**, *5*, 871–879. (b) Kempe, K.; Lobert, M.; Hoogenboom, R.; Schubert, U. S. *J. Polym. Sci., Part A: Polym. Chem.* **2009**, *47*, 3829–3838.
- (4) (a) Uyama, H.; Kobayashi, S. *Chem. Lett.* **1992**, 1643–1646. (b) Park, J.-S.; Kataoka, K. *Macromolecules* **2007**, *40*, 3599–3609. (c) Hoogenboom, R.; Thijs, H. M. L.; Jochems, M. J. H. C.; Van Lankvelt, B. M.; Fijten, M. W. M.; Schubert, U. S. *Chem. Commun.* **2008**, 5758–5760.
- (5) Bloksma, M. M.; Weber, C.; Perevyazko, Y.; Kuse, A.; Baumgärtel, A.; Vollrath, A.; Hoogenboom, R.; Schubert, U. S. *Macromolecules* **2011**, *44*, 4057–4064.
- (6) (a) Wiesbrock, F.; Hoogenboom, R.; Abeln, C. H.; Schubert, U. S. *Macromol. Rapid Commun.* **2004**, *25*, 1895–1899. (b) Wiesbrock, F.; Hoogenboom, R.; Leenen, M. A. M.; Meier, M. A. R.; Schubert, U. S. *Macromolecules* **2005**, *38*, 5025–5034.

- (7) Kobayashi, S.; Tokuzawa, T.; Saegusa, T. *Macromolecules* **1982**, *15*, 707–710.
- (8) Miyamoto, M.; Aoi, K.; Saegusa, T. *Macromolecules* **1988**, *21*, 1880–1883.
- (9) Lobert, M.; Köhn, U.; Hoogenboom, R.; Schubert, U. S. *Chem. Commun.* **2008**, 1458–1460.
- (10) De Proft, F.; Langenaeker, W.; Geerlings, P. *Tetrahedron* **1995**, *51*, 4021–4032.
- (11) (a) Lee, C. T.; Yang, W. T.; Parr, R. G. *Phys. Rev. B* **1988**, *37*, 785–789. (b) Becke, A. D. *J. Chem. Phys.* **1993**, *98*, 5648–5652.
- (12) (a) Zhao, Y.; Truhlar, D. G. *Theor. Chem. Acc.* **2008**, *120*, 215–241. (b) Liu, L.; Malhotra, D.; Paton, R. S.; Houk, K. N.; Hammond, G. B. *Angew. Chem., Int. Ed.* **2010**, *49*, 9132.
- (13) (a) Hratchian, H. P.; Schlegel, H. B. *J. Chem. Phys.* **2004**, *120*, 9918. (b) Hratchian, H. P.; Schlegel, H. B. *J. Chem. Theory Comput.* **2005**, *1*, 61–69. (c) Fukui, K. *Acc. Chem. Res.* **1981**, *14*, 363–368.
- (14) Boys, S. F.; Bernardi, F. *Mol. Phys.* **1970**, *19*, 553–566.
- (15) Frisch, M. J., et al. *Gaussian 09*, Revision B.01; Gaussian, Inc.: Wallingford, CT, 2010.
- (16) (a) Parr, R. G.; Yang, W. *Density-Functional Theory of Atoms and Molecules*; Oxford Science Publications, 1988. (b) Geerlings, P.; De Proft, F.; Langenaeker, W. *Chem. Rev.* **2003**, *103*, 1793–1873. (c) Hemelsoet, K.; Van Speybroeck, V.; Waroquier, M. *Chem. Phys. Lett.* **2007**, *444*, 17–22.
- (17) (a) Pearson, R. G. *Acc. Chem. Res.* **1993**, *26*, 250–255. (b) Zhou, Z. X.; Parr, R. G. *J. Am. Chem. Soc.* **1990**, *112*, 5720–5724.
- (18) Ayers, P. W.; Parr, R. G.; Pearson, R. G. *J. Chem. Phys.* **2006**, *124*, 194107.
- (19) (a) Parr, R. G.; Yang, W. *J. Am. Chem. Soc.* **1984**, *106*, 4049–4050. (b) Ayers, P. W.; Levy, M. *Theor. Chim. Acta* **2000**, *103*, 353–360. (c) Catak, S.; D'hooghe, M.; Verstraelen, T.; Hemelsoet, K.; Van Nieuwenhove, A.; Ha, H.-J.; Waroquier, M.; De Kimpe, N.; Van Speybroeck, V. *J. Org. Chem.* **2010**, *75*, 4530–4541.
- (20) (a) Bultinck, P.; Ayers, P. W.; Fias, S.; Tiels, K.; Van Alsenoy, C. *Chem. Phys. Lett.* **2007**, *444*, 205–208. (b) Van Damme, S.; Bultinck, P.; Fias, S. *J. Chem. Theory Comput.* **2009**, *5*, 334–340. (c) Verstraelen, T.; Van Speybroeck, V.; Waroquier, M. *J. Chem. Phys.* **2009**, *131*, 044127–19.